

## NEUTRINO INTERACTIONS



R.D. Ransome  
*Rutgers The State University of New Jersey,  
 Piscataway,  
 NJ,  
 08854,  
 USA*

The advent of very high intensity neutrino beams for the study of neutrino oscillations has also made possible a new generation of experiments which will study neutrino interactions on different nuclei with unprecedented precision. The use of the neutrino as a probe of nucleon structure provides unique information not available with other probes. In addition, an improved understanding of the neutrino interaction cross section and the resulting final states will reduce systematic uncertainties in neutrino oscillation experiments. A review of recent interaction measurements for neutrino energies in the energy range of 500 MeV to a few GeV will be given, with an emphasis on quasi-elastic scattering.

## I. INTRODUCTION

The discovery of neutrino oscillations has opened a new era of neutrino physics. Very intense neutrino beam lines have been built at CERN, JPARC, and Fermilab in the past decade with the goal of studying neutrino oscillations in detail. These cover a wide range of energies, from less than 1 GeV for the MiniBooNE, SciBooNE (Fermilab)[1], and T2K (JPARC)[2] experiments, to peak energies of a few GeV with long tails up to greater than 50 GeV for the NuMI (Fermilab)[3] and CNGS (CERN)[4] beam lines. Accurate interpretation of oscillation experiments, and a thorough understanding of the systematic uncertainties of the measurements, requires knowledge of both inclusive cross sections and details of final state characteristics. Experiments have been designed to improve those measurements. However, neutrino beams are so intense that they have also opened possibilities for using the neutrino as a scattering probe to explore nucleon structure and to study the interaction of neutrinos with nuclei with unprecedented detail. It is this aspect of neutrino interactions that I want to concentrate on in this report.

The neutrino has many attractive aspects as a scattering probe. It interacts only through the well understood weak interaction which makes it an ideal probe of the weak structure of the nucleon. It has a unique flavor sensitivity and, by combining neutrino and antineutrino scattering, provides flavor separation not

available by any other means. Unfortunately it has a number of unattractive aspects. The incoming neutrino cannot be tracked, nor can the outgoing neutrino for neutral current interactions be tracked. Even with the intense beams currently available, massive targets (typically many tons) are needed to get adequate rates. The incident neutrino energy for any particular interaction is not known, and beams have a broad range of energies for on axis beams, and even off axis beams have significant (over 100 MeV) widths. Finally, interpretation of any results require detailed Monte Carlo simulations, and the validity of those simulations depends on the accuracy of the input data.

The fact that the incident neutrino energy is not known for any particular interaction is of importance for oscillation experiments because the critical oscillation parameter is  $L/E$  (distance over energy). The energy is inferred from the energy and angle of the final state muon (for charged current interactions), along with observed energy of the other final state particles. Because the interaction nucleus is typically carbon or heavier nuclei, energy can be unobserved because of binding energy, final state neutrons, or other particles not well measured. This aspect is what makes understanding the final state characteristics so important to oscillation experiments.

Prior to the recent series of experiments, most cross section data were taken with bubble chambers. Very little data existed for at lower energies, especially for heavier targets. A summary of neutrino total cross

sections is shown in Fig. 1. As is clearly evident, statistics are poor for neutrino energies of less than a few GeV.

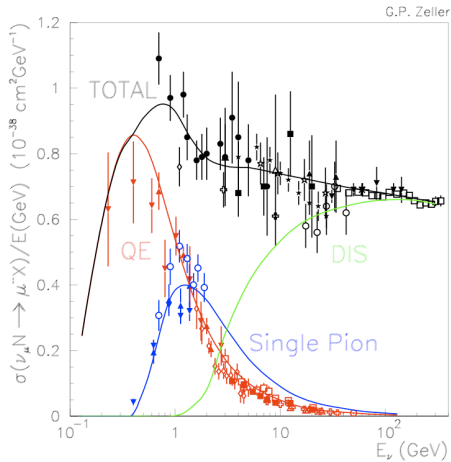


FIG. 1: Summary of cross sections measurements prior to 2006. Plot courtesy of G. Zeller[6]

A rather complete summary of neutrino interactions was given at PIC2010[5], including a discussion of higher energy measurements. In this talk I will concentrate on recent measurements of the quasi-elastic cross section at lower energies, and some data on coherent scattering.

## II. QUASI-ELASTIC SCATTERING

### A. Background

Quasi-elastic scattering refers to the charged current interaction  $\nu n \rightarrow \mu^- p$  or  $\bar{\nu} p \rightarrow \mu^+ n$ . The reaction is of interest for several reasons. It is important for oscillation experiments because it has the best measure of the neutrino energy. For a true two body interaction, the neutrino energy can be determined from the muon kinematics alone. If the interaction occurs in a nucleus, fermi momentum, the binding energy and final state interactions smear and shift the estimated energy, but it still remains the best measure of the incident neutrino energy. For higher neutrino energies, above a few GeV, the quasi-elastic cross section is nearly constant and can thus serve as a measure of the neutrino flux. For experiments using neutrino energies below one GeV, such as MiniBooNE and T2K, the quasi-elastic interaction is the dominant part of the cross section.

The reaction is of intrinsic interest for studying the nucleon because it is the best way to determine the weak form factor of the nucleon. The neutrino-nucleon cross section can be written as a function of the vector form factors and the axial form factor. The vector

form factors are taken from electromagnetic scattering:

$$\frac{d\sigma}{dQ^2} = \frac{M^2 G_F^2 \cos^2(\theta_c)}{8\pi E_\nu^2} [A - B(s-u) + C(s-u)^2]$$

where A, B, and C are functions of the electromagnetic and axial form factors,  $s$  and  $u$  are the usual Mandelstam variables,  $M$  is the nucleon mass,  $G_F$  is the Fermi constant,  $\theta_c$  is the Cabbibo angle, and  $E_\nu$  is the neutrino energy. Except for the neutron electric form factor, which is small and has a different functional form, the nucleon form factors are approximately described by the same functional form:

$$G_{E,M,A}(Q^2) = \frac{G(0)}{(1 + Q^2/M_{V,A}^2)^2}$$

where E, M, and A designate the electric, magnetic, and axial form factors, and  $M_{V,A}$  is a parameter called the vector or axial mass. Although, the dipole form for the form factors is empirical, and there is no particular physical significance to the vector or axial mass, the form does have the correct behavior expected from perturbative QCD for very large  $Q^2$ .

### B. Axial Form Factor

In the functional form given above, the vector form factors are determined from electron scattering and the  $Q^2 = 0$  value for  $G_A$  is determined from neutron beta decay, leaving only one free parameter to fit the  $Q^2$  distribution for neutrino scattering: the axial mass  $M_A$ . Prior to the 1990's, most determinations of the axial mass were done using neutrino scattering on deuterium or hydrogen targets. Although the statistical uncertainties were typically 10-20%, the experiments were in generally good agreement with a world average for  $M_A$  of about 1.03.

In the 1990's one of a new generation of oscillation experiments, NOMAD[7], measured the axial form factor as part of its studies[8] for neutrino and antineutrino scattering with energies between 5 and 100 GeV. The tracking detectors also served as the scattering target and consisted of a mixture of elements, but were primarily carbon. As can be seen in Fig. 2, the quasi-elastic cross section and extracted axial mass were in generally good agreement with previous measurements.

The next generation of oscillation experiments took place at Fermilab in the Booster Neutrino Beamline, with neutrino energies between about 0.5 and 1 GeV. The first experiment, MiniBooNE, was designed to check the LSND experiment. LSND observed oscillation values which, combined with other oscillation results, would imply sterile neutrinos. The MiniBooNE

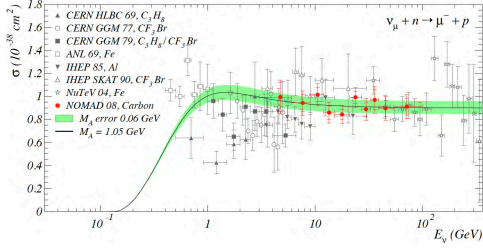


FIG. 2: Axial mass as determined in the NOMAD experiment, along with previous data.

detector consisted of a 6.1 m diameter tank of mineral oil ( $\text{CH}_2$ ) viewed by 1280 eight-inch phototubes. Because intrinsic impurities present in mineral oil scintillate, both Cerenkov light and scintillation light were detected.

A second detector, SciBooNE, was added on the same beam line later. The SciBooNE detector was originally used at KEK (called SciBar). The detector consists of 14,436 strips of plastic scintillator (CH), each 1.3 cm x 2.5 cm x 300 cm, with wavelength shifting fiber readout. It was moved to the Booster Neutrino Beamline in 2007 and an electromagnetic calorimeter and muon range stack were added.

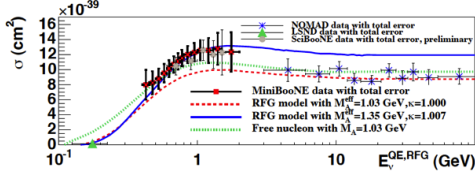


FIG. 3: Axial mass as determined by MiniBooNE and SciBooNE, along with the NOMAD data.

Both MiniBooNE and SciBooNE were able to extract the axial mass in the lower energy range, and both primarily from carbon[9, 10]. As seen in Fig. 3, the MiniBooNE and SciBooNE data are in good agreement with each other. However, the best fit to the data required a substantially higher value of  $M_A$ , of about 1.35 GeV. This gives a significant discrepancy with the higher energy data. The form factor cannot depend on the incident neutrino energy, so the difference must be due to some other effect. Other more recent experiments have also found values of  $M_A$  that are higher than previous measurements, as shown in Fig. 4. The one common characteristic of the later experiments with higher values of  $M_A$  is that they were done at lower energy and with heavier nuclear targets (i.e. not deuterium). A possible solution of this discrepancy may reside in the issues with the electromagnetic form factors or nuclear effects at low energy.

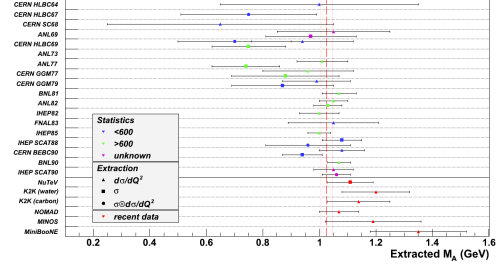


FIG. 4: Experimental measurements of the axial mass[11].

### C. Nuclear effects and the electromagnetic form factors

The history of the determination of the electromagnetic form factors provides some interesting lessons for the determination of the axial form factor. Early measurements showed good agreement with the dipole form of the form factor, with a vector mass of 0.84 GeV. Both the electric and magnetic form factors of the proton appeared to have the same form, and the ratio appeared to be nearly constant with  $Q^2$ . However, beginning in the late 1990's, a series of experiments using polarization transfer to determine the form factor ratio showed deviations from the dipole form even at low  $Q^2$ , and a substantial change in the ratio of the electric to magnetic form factors as  $Q^2$  increased[12]. Figure 5 shows a global fit to the world's data. The important point to be noticed here is that as  $Q^2$  gets larger than 1 GeV<sup>2</sup>, both  $G_E$  and  $G_M$  have significant deviations (about 10% by  $Q^2$  of 2 GeV<sup>2</sup>) from the dipole form. As measurements of the axial form factor become more precise, especially at higher  $Q^2$ , potential deviations from the dipole form will have to be taken into account.

The electromagnetic form factors have been determined from electron scattering from hydrogen targets. Similar measurements were also made using the polarization technique for the reaction  ${}^4\text{He}(\vec{e}, e'\vec{p}){}^3\text{H}$ [14]. As is shown in Fig. 6, the ratio differs from one by several percent. Much of the difference is explained from conventional nuclear effects. However, conventional models plus a modification of the nucleon form in the nuclear medium as predicted by Saito *et al.*[15] gives a better fit to the data.

The model from Ref. [15] also predicts modification of the axial form factor, at the level of 10% for  $Q^2$  less than 1 GeV<sup>2</sup>. However, the model predicts a *smaller* value of  $G_A$  in the medium, which is opposite of the apparent effect observed by MiniBooNE/SciBooNE. The question of a medium modification of the EM and axial form factors is still open, and needs to be taken into account when extracting form factors from the nucleons in the nuclear medium.

Finally, another nuclear effect, which has been con-

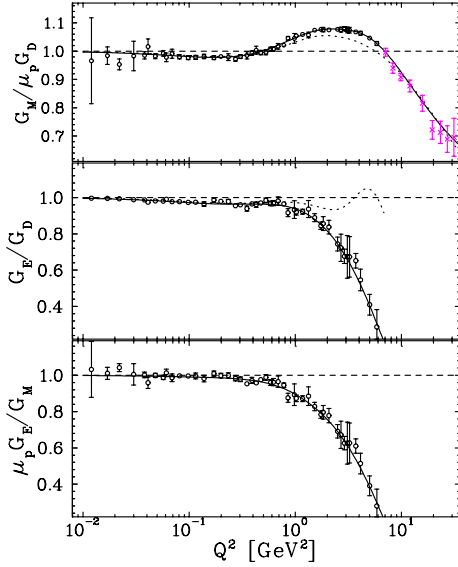


FIG. 5: Proton electromagnetic form factors from Ref. [13].

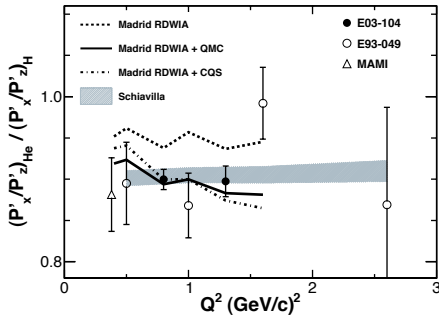


FIG. 6: Ratio of polarization transfer for the  ${}^4\text{He}(\vec{e}, e'\vec{p}){}^3\text{H}$  reaction compared to  ${}^1\text{H}(\vec{e}, e'\vec{p})$ [14]. The ratio is sensitive to medium modifications of the proton form factor.

firmed over the last decade, is the enhancement of the transverse nuclear response compared to the free nucleon in inclusive electron scattering[16]. The enhancement is attributed to meson exchange currents and short range correlations, and is present even in  ${}^4\text{He}$ , at about the same level as in heavier nuclei. Bodek *et al.*[17] have shown that the enhancement can be modeled as an effective change of the nucleon magnetic form factor in nuclei. The effect is most pronounced at low  $Q^2$  and causes an increase in the cross section compared to expectations from using the free form factors. As the neutrino energy increases, the maximum  $Q^2$  increases, and the value of  $M_A$  needed to fit the data moves toward the free values. As shown in Fig. 7, the model provides a good description of both the low and high energy data, and appears to resolve the inconsistency between the two.

To conclude this section, we see that the most recent experiments, with their much improved statistics,

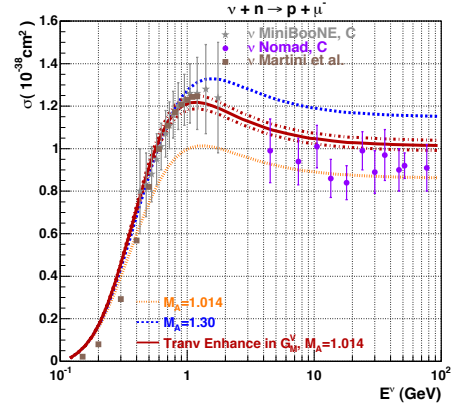


FIG. 7: Cross section predictions of the transverse enhancement model of Bodek *et al.*[17]. The model predicts the increased cross section for neutrino energies near 1 GeV compared to scattering from deuterium, as well as the decrease as the neutrino energy increases.

have brought new interest to an old topic. Neutrino scattering experiments have reached the stage of needing good models of nuclear effects as well as potentially giving new information on the nuclear medium effects on the structure of the nucleon. Proper accounting for nuclear effects is a challenging theoretical problem and even for the simpler case of electron scattering is not fully resolved. High statistic neutrino scattering will no doubt provide even more challenges to theory.

### III. COHERENT PION PRODUCTION

The second experimental result which has become of considerable interest is coherent pion production. Coherent pion production refers the reaction  $\nu + A \rightarrow \nu + \pi^0 + A$  (neutral current production) and  $\nu + A \rightarrow \mu^- + \pi^+ + A$  (charged current production). In each case, the neutrino interacts with the entire nucleus, leaving it in the ground state, with a single pion produced. The kinematics of these interactions give very little recoil energy to the nucleus, and the pion production is forward peaked. As with the quasi-elastic scattering, this reaction has a particular interest for oscillation experiments, as well as being an intrinsically interesting reaction.

Coherent pion production is a potentially large background for oscillation experiments. Neutral current production in particular is of a concern for experiments searching for electron neutrino appearance (such as NOvA[18]) because the photon showers from a  $\pi^0$  decay can easily be confused with an electron shower if one photon either escapes detection or the two are too close to be distinguished.

A number of models[20] exist which predict the coherent pion production cross section, and the charged current to neutral current ratio, although the most widely used is the Rein-Sehgal (RS) model[21]. Recent reviews of the theoretical status and comparison of models can be found in Refs. [22] and [23]. Coherent pion production has been measured at higher energies by the MINOS experiment at Fermilab[19, 24], and those data are in reasonable agreement with RS, as shown in Fig. 8.

K2K[25] set the first limit on CC coherent production near 1.2 GeV. They found no evidence for this channel, with an upper limit of  $0.6 \times 10^{-2}$  for the ratio of CC coherent to total CC interactions, below the prediction of RS of about  $1 \times 10^{-2}$ . SciBooNE[26] has observed NC coherent production at the level of  $1.1 \times 10^{-2}$ , in approximate agreement with RS, but they also found CC coherent to be suppressed, with a CC/NC ratio of only  $0.14^{+0.30}_{-0.28}$ . RS and other recent models[27] predict a ratio of CC/NC to be 1 to 2. This rather large discrepancy between models and data remains a mystery.

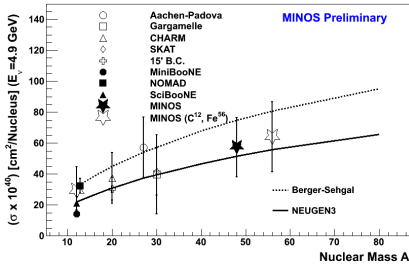


FIG. 8: MINOS coherent production cross section.

#### IV. EXPERIMENTS

As we have seen above, the most recent experiments have given results which appear inconsistent with previous experiments and have placed new demands on theoretical explanations, in particular on nuclear dependence of effects. There is a need for more precise measurements and studies of nuclear effects, especially at energies below a few GeV. In this section I want to discuss two new experiments which significant potential to improve the experimental situation: MINERvA, at Fermilab, and T2K at JPARC.

##### A. MINERvA

MINERvA[28, 29] is a high resolution neutrino cross section experiment in the NuMI beam line at Fermilab, upstream of the MINOS near detector. The goal

of the experiment is to measure exclusive and inclusive neutrino cross sections in the energy range of 1-20 GeV on several nuclei with greatly improved precision over previous experiments. MINERvA will be able to address several issues raised above. It will span the energy range between MiniBooNE and NOMAD, allowing a study of the extracted  $M_A$  as a function of energy and on different nuclear targets, which will allow a study of the possible nuclear effects in the extraction of  $M_A$ . It will also have good sensitivity to CC coherent production over the range of neutrino energies where models appear to fail.

A schematic of the MINERvA detector is shown in Fig. 9. The detector consists of five main regions: the fully active central detector, the upstream nuclear targets, a downstream electromagnetic and hadron calorimeter, and a surrounding electromagnetic and hadron calorimeter.

The central detector serves as both the primary target and the tracking detector. It consists of planes of triangular plastic scintillator strips arranged in three orientations. Each strip's triangular cross section is 1.7 cm high and 3.3 cm wide, and is read out via a wavelength shifting fiber. The strips range from about 1 m to 2 m in length. Light sharing between the strips gives a position resolution of approximately 3 mm. The light yield is approximately 5.0 photo-electrons/MeV, giving about 13.5 photo-electrons/plane for minimum ionizing muons.

The downstream electromagnetic calorimeter consists of alternating planes of 2 mm thick Pb and scintillator planes of the same hexagonal shape as in the central detector. The hadron calorimeter is similar, with 2.5 cm planes of steel instead of Pb. The side electromagnetic calorimeter consists of 2 mm thick Pb plates between tracking plane in the outer region of the central detector. The side hadron calorimeter consists of planes of steel with scintillator strips embedded.

Upstream of the central detector are planes of passive targets, with two planes 2.5 cm thick of mixed Fe/Pb, one plane with 2.5 cm thick Fe/Pb and 7.5 cm C, a solid plane of Pb 0.80 cm thick, and a mixed plane of Fe/Pb 1.30 cm thick. The mixed Fe/Pb planes are split with part of the plane being iron and part of the plane being lead, such that the total mass is approximately equal. Tracking planes are placed between each plane of passive targets. Planned for fall 2011 are a 15 cm water target to be installed downstream of the Fe/Pb/C target and a tank of liquid 4He about 1 m in diameter to be installed upstream of the main detector. Figure 10 shows a schematic of the nuclear target region along with the placement of carbon, lead, and iron in the various targets.

Charged current events originating in the central detector are fully contained, except for the muon, for neutrino energies of less than about 10 GeV. The MINOS detector gives both muon energy and charge for

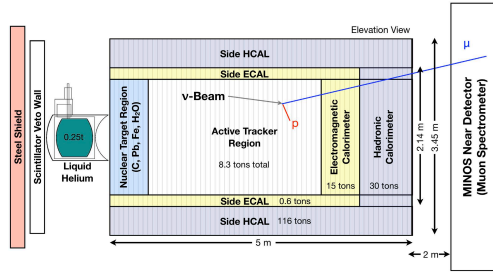


FIG. 9: Schematic side view of the MINERvA detector.

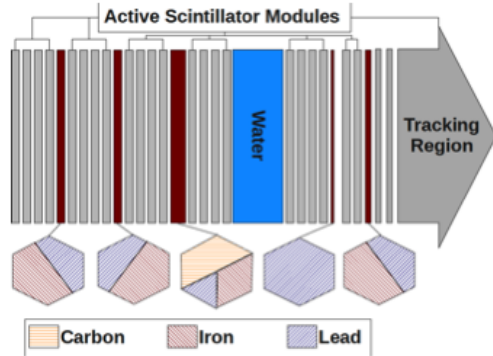


FIG. 10: Nuclear target region of the MINERvA detector.

forward going muons. The threshold energy for a muon to exit MINERvA and be tracked into MINOS is about 2 GeV. There is good angular acceptance for muons with scattering angles below 10 degrees, with acceptance dropping to zero for scatters greater than about 20 degrees. For particles stopping in MINERvA particle identification can be determined from the  $dE/dX$ , but there is no charge determination.

MINERvA began operations with about half of the detector installed in November, 2009, and took data with the anti-neutrino beam until March, 2010. Installation of the full detector was completed in March, 2010. Running since that time has been divided between the neutrino mode, anti-neutrino mode, along with a few special settings intended to help determine the neutrino flux. The analysis to date has concentrated on those events which have a muon identified in MINOS. Two of the first analyses are of the A dependence of the inclusive cross section and of the quasi-elastic anti-neutrino cross section.

MINERvA will be able to determine the nuclear dependence of the inclusive cross section, and in particular the relative ratio of lead, iron, and carbon. Although the statistical precision will be quite good, better than 1%, the measurement requires a precise determination of the actual interaction nucleus in a given interaction. The transverse resolution of the de-

tektor is quite good, and Monte Carlo simulations indicate that fewer than 0.1% of vertices will be tracked to the wrong target. The longitudinal resolution is less precise and depends on the number of final state particles and how far they travel. Because there is no tracking in the Fe/Pb targets, it is not possible to tell if events with a single muon in the final state originated in Pb/Fe target or in the downstream tracking detectors. Monte Carlo studies of the background do indicate that it is substantial, as shown in Fig. 11.

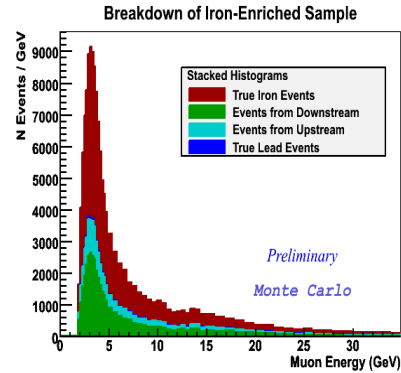


FIG. 11: A Monte Carlo estimate of the relative number of events tracked to the iron target vs. the actual vertex location.

A measurement of the cross section in iron requires subtraction of the background from scintillator. The cross section on scintillator can be determined from the tracking detectors, and is currently underway. In addition to the background subtraction, an acceptance correction must be made. The acceptance of muons from the Pb and Fe targets is not identical, so a precise measurement of the Fe/Pb ratio requires a precise acceptance correction, which is done with the Monte Carlo simulation. The Monte Carlo has been checked by comparing data from regions of scintillator with the same areas as the Fe/Pb just downstream of the target, and comparing with Monte Carlo estimates. There is good agreement between data and Monte Carlo, as shown in Fig. 12. Analysis of the data to determine the Pb/Fe inclusive ratio is still underway.

The anti-neutrino quasi-elastic scattering was measured in the first running period with the partial detector. Figure 13 shows the  $Q^2$  distribution for all energies combined compared to a Monte Carlo simulation of the components of the measured cross section, with the Monte Carlo results normalized to the data. The preliminary data are in general agreement with an axial mass of 1.05. However, studies of the absolute neutrino flux, as well as further analysis of the scattering data, are still underway. The statistics of the data shown are only about one-eighth of the total anticipated anti-neutron data, and 1/30 of the

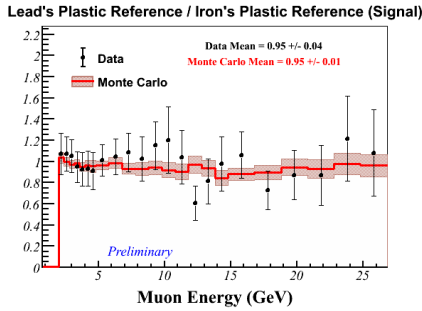


FIG. 12: The ratio of the iron-like to lead-like regions of the tracking detectors as a function of muon energy, compared to Monte Carlo.

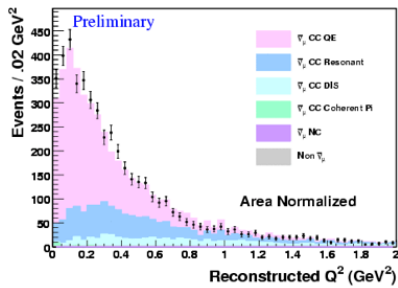


FIG. 13: Anti-neutrino quasi-elastic cross section compared to a Monte Carlo estimate, summed over all neutrino energies. The Monte Carlo is area normalized to the data.

total neutrino data anticipated. The precision, especially at higher  $Q^2$ , will make it possible to compare the shape of the axial form factor to the dipole form for the first time.

## B. T2K

A second experiment which will substantially improve our knowledge of low energy interaction cross sections is T2K at JPARC. Although primarily designed to measure the  $\theta_{13}$  oscillation parameter, T2K also has a near detector, called the ND280 detector. A schematic of the detector is shown in Fig. 14. ND280 includes an upstream  $\pi^0$  detector (P0D), consisting of interleaved scintillator and water targets, designed to measure  $\pi^0$  production in water. Downstream of the P0D are fine grained scintillator detectors, consisting of 1 cm square scintillator bars which are used as active neutrino targets, interleaved with time projection chambers (TPCs) for particle identification. The inner detectors are surrounded by electromagnetic calorimetry and the entire assembly is contained inside the former CERN UA1 magnet, which provides a nominal 0.2 T field. A sample event is shown in Fig. 15.

The ND280 detector is 2.5 degrees off axis of the neutrino beam, giving a peak energy of about 600 MeV with a FWHM of about 400 MeV. This relatively low energy and relatively narrow beam, coupled with the very good  $\pi^0$  detection, excellent tracking, charged particle identification and good energy measurements provided by the FGD will allow T2K to study neutrino interactions carbon and oxygen for sub-GeV neutrino energy with unprecedented precision.

T2K began data taking in early 2010 and continued until neutrino production stopped following the Fukushima earthquake in March 2011. Data taking should begin again in early 2012.

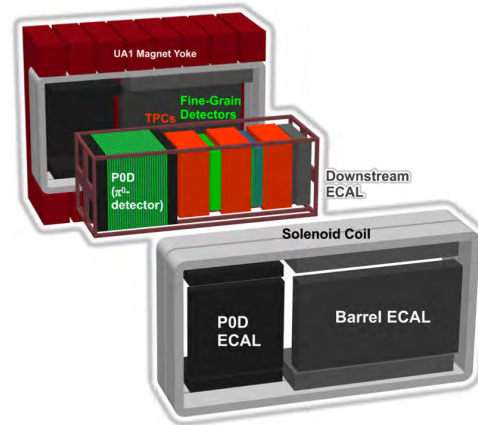


FIG. 14: T2K near detector.

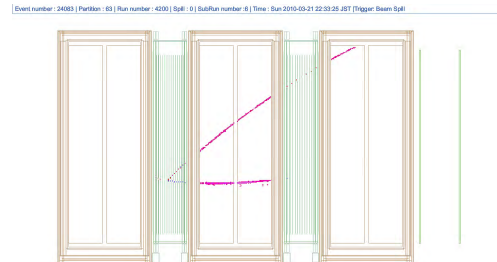


FIG. 15: T2K two track event in ND280 detector.

## V. SUMMARY

A new generation of high intensity neutrino beams and fine grained detectors have made possible the use of the neutrino as a probe of nucleon structure. As the precision of measurements has increased, significant discrepancies between the data from different experiments as well as comparisons between data and theoretical predictions. The understanding of neutrino interactions in nuclei has become increasingly important, and will be addressed by new high precision experiments in the coming years.

### Acknowledgments

This work supported by the US National Science Foundation and the US Dept. of Energy. I would

like to thank the MINERvA collaboration, the T2K collaboration, B. Berger, M. Wascko, R. Petti, and G. Zeller for assistance with this presentation.

- 
- [1] BooNE website: <http://www-boone.fnal.gov/>
  - [2] JPARC website: <http://j-parc.jp/index-e.html>
  - [3] NuMI website: <http://www-numi.fnal.gov/>
  - [4] CNGS website: <http://proj-cngs.web.cern.ch/proj-cngs/>
  - [5] M. Wilking, Physics in Collision, Proceedings, 30th International Conference, PIC 2010, Karlsruhe, Germany, J. Komaragiri, T. Muller, J. Wagner-Kuhr (editors) 190, 2011.
  - [6] G. Zeller, arXiv:hep-ex/0312061 (2003).
  - [7] J. Altegoer, *et al.*, Nucl. Inst. Meth. **A404**, 96 (1998).
  - [8] V. Lyubushkin *et al.*, Euro. Phys. J. C **63** 355 (2009).
  - [9] A.A. Aguilar-Arevalo, Phys. Rev. D **81**, 092005 (2010).
  - [10] M.O. Wascko, Nucl. Phys. B Suppl. **00**, 1 (2011), J. Alcaraz and J. Walding, arXiv:0909.564 [hep-ex] (2009).
  - [11] Figure courtesy B. Ziemer, UC Irvine.
  - [12] See A.J.R. Puckett, *et al.*, Phys. Rev. Lett. **104**, 242301 (2010), G. Ron, *et al.*, Phys. Rev. Lett. **99**, 202002 (2007), and C.F. Perdrisat, V. Punjabi, M.Vanderhaeghen, Prog. Nucl.Part. Phys. **59**, 694 (2007) and references therein.
  - [13] J. Arrington, W. Melnitchouk, J.A. Tjon, Phys. Rev. C **76**, 035205 (2007).
  - [14] M. Paolone, *et al.*, Phys. Rev. Lett. **105**, 072001 (2010).
  - [15] K. Saito, K. Tsushima, and A.W. Thomas, Prog. Part. Nucl. Phys. **58**, 1 (2007).
  - [16] J. Carlson, J. Jourdan, R. Schiavilla, and I. Sick, Phys. Rev. C **65**, 024002 (2002).
  - [17] A. Bodek, H.S. Budd, and E. Christy, arXiv:1106.0340[hep-ph], and Eur. Phys. J. C **71**, 1726 (2011).
  - [18] Website: <http://www-nova.fnal.gov/>
  - [19] See <http://www-numi.fnal.gov/> for a description of the MINOS experiment.
  - [20] S.S. Gershtein, Yu.Ya.Komachenko, M.Y. Khlopov, Sov. J. Nucl. Phys. **32**, 861 (1980); Yu.Ya. Komachenko and M.Yu. Khlopov, Sov. J. Nucl. Phys. **45**, 295 (1987); B.Z. Kopeliovich and P. Marage, Int. J. Mod. Phys. **8** 1513 (1993); S.K. Singh, M.S. Althar, S. Ahmad, Phys. Rev. Lett. **96**, 241801 (2006); E.A. Paschos, A. Kartavtsev, and G.J. Gounaris, Phys. Rev. D **74**, 054007 (2009); C. Berger and L.M. Sehgal, Phys. Rev. D **79**, 053003 (2009); M. Martini, M. Ericson, G. Chanfray, and J. Marteau, Phys. Rev. C **80**, 065501 (2009); E. Hernandez, J. Nieves, and M.J.V. Vascas, Phys. Rev. D **80**, 013003 (2009); S.X. Nakamura, *et al.*, Phys. Rev. C **81**, 035502 (2010).
  - [21] D. Rein and L.M. Sehgal, Ann. Phys. **133**, 79 (1981), D. Rein and L.M. Sehgal, Nucl. Phys. **B223**, 29 (1983), D. Rein and L.M. Sehgal, Phys. Lett. B **657**, 207 (2007).
  - [22] L. Alvarez-Ruso, NuInt11 proceedings (to be published) and [www.nuint11.in](http://www.nuint11.in).
  - [23] S. Boyd, *et al.* in AIP Conf. Proceedings 1189, F. Sanchez, M. Sorel, L. Alvarez-Ruso, A. Cervera, M. Vicente-Vacas, eds., (Melville, NY) 60.
  - [24] D. D. Cherdack, [lss.fnal.gov/archive/thesis/fermilab-thesis-2010-54.pdf](http://lss.fnal.gov/archive/thesis/fermilab-thesis-2010-54.pdf) and D.D. Cherdack, NuInt11 presentations, <http://nuint11.in/>
  - [25] M. Hasegawa, *et al.*, Phys. Rev. Lett. **95**, 252301 (2005).
  - [26] Y. Kuitmoto, *et al.*, Phys. Rev. D **81**, 111102(R) (2010).
  - [27] E. Hernandez, J. Nieves, M.Valverde, Phys. Rev. D **82**, 077303 (2010).
  - [28] MINERvA collaboration members listed at <http://minerva.fnal.gov/>.
  - [29] R.D. Ransome, PANIC 2011 proceedings, to be published.
  - [30] B. Berger, PANIC 2011 proceedings, to be published, and V. Paolone and S. Dytman, T2K-PROC-008, [www.t2k.org/docs/proc/index.html](http://www.t2k.org/docs/proc/index.html).